

Adsorbate-Induced Reconstruction in the Ni(110)-H System

Y. Kuk, P. J. Silverman, and H. Q. Nguyen^(a)

AT&T Bell Laboratories, Murray Hill, New Jersey 07974

(Received 10 July 1987)

The adsorbate-induced reconstruction of the room-temperature Ni(110)-H surface has been resolved by scanning tunneling microscopy. The structure, known as a "streaky" (1×2) from LEED observations, is found to be primarily a (5×2) Ni reconstruction with small domain size along the $\langle 001 \rangle$. Top-layer Ni atoms are paired along the $\langle 001 \rangle$ by a 0.5-\AA lateral displacement to form tetramers and every fifth $\langle 001 \rangle$ row is missing. The barrier height, measured simultaneously with a constant-current topograph, is found to be higher along the $\langle 001 \rangle$ missing rows.

PACS numbers: 68.35.Ja, 61.16.Di, 68.45.Da, 73.40.Gk

Many surfaces undergo reconstruction in the presence of adsorbates¹ in order to lower their surface energy. The chemisorption of hydrogen on transition-metal surfaces is of particular interest for its role in catalysis and as a simple case of the general chemisorption phenomenon.² Extensive studies³⁻¹⁶ of hydrogen adsorption on Ni(110) have produced conflicting results on the structure of the surface. In this Letter, we show the first direct image produced by scanning tunneling microscope (STM) of a substrate reconstruction induced by hydrogen. Individual nearest-neighbor atoms with a lateral separation of 2.5 \AA were resolved. The structure observed by STM can explain some of the puzzling results obtained by other experimental techniques.

Six different reconstructions of the Ni(110)-H system have been observed by LEED (low energy electron diffraction)⁶ and He diffraction⁷: (2×1) , (2×6) , $c(2 \times 4)$, $c(2 \times 6)$, (1×2) , all below 220 K, and "streaky" (1×2) at room temperature. The first four low-temperature structures, produced by H coverages < 1 monolayer, were interpreted as unreconstructed substrates with the adsorbate exhibiting long-range order, i.e., lattice-gas systems. The weakness of the fractional-order LEED spots seems to confirm this model, with support from thermal desorption⁸ and electron-energy-loss spectroscopy^{9,10} measurements. The low-temperature (1×2) structure, studied by LEED,^{5,6,12} He diffraction,⁷ and high-energy ion scattering with nuclear-reaction analysis,¹³ has been variously ascribed to missing $\langle 1\bar{1}0 \rangle$ rows¹² or to a "row pairing" distortion of the topmost layer of Ni atoms^{4,11,13,14} with lateral displacement of 0.1 \AA . At 220 K, the structure undergoes an irreversible transition to a streaky (1×2) phase, which can also be produced by hydrogen exposure of the clean Ni(110) at room temperature. There have been conflicting reports about the similarity of the low-temperature (1×2) and the streaky (1×2) structures. An electron-energy-loss spectroscopy study¹⁰ proposed a model in which the streaky (1×2) phase is a mixture of disordered areas and low-temperature (1×2) and (2×1) phases. A LEED study¹⁵ has suggested that there is a range of displacements of the

paired Ni atoms at room temperature, while the lateral displacement is 0.1 \AA for all pairs at low temperature. The surface peak measurement by ion channeling¹³ at low temperature has shown that the displacement of all the paired Ni atoms is 0.1 \AA , while only 20% of the topmost Ni atoms are displaced by that amount at room temperature. However, a recent room-temperature ion-channeling study¹⁶ proposed a model in which the paired Ni atoms are displaced by 0.5 \AA , and the H atoms are located 0.09 \AA away from the short bridge site. In this study, we have found the structure to be quite different from this proposed model, although the displacement of the paired Ni atoms is in agreement.¹⁶

A detailed description of the STM¹⁷ used in the present study can be found elsewhere.¹⁸ Briefly, an ultrahigh-vacuum chamber is equipped with STM, LEED, and Auger-electron spectroscopy to study the sample surface and a field ion microscope to characterize the STM tip. A clean Ni(110)- (1×1) surface was prepared by ion sputtering and annealing until no trace of impurities was detected by Auger-electron spectroscopy. The streaky (1×2) phase was then formed by exposure of H_2 for $< 2\text{ L [1 L (langmuir) = }10^{-6}\text{ Torr sec]}$ at room temperature. H_2 is known to chemisorb dissociatively on Ni surfaces, forming atomic hydrogen bonds, so that excitation by a hot filament is unnecessary. Since H_2 also readily adsorbs onto W, the STM tip was cleaned by field evaporation after the exposure.

STM topographs were taken with a tip bias of $+2$ to -2 V and a constant tunneling current of less than 100 pA . Figure 1 is a $240 \times 190\text{-\AA}^2$ STM topograph of the Ni(110)-H surface. The crystallographic directions were determined by the LEED pattern, and the X and Y piezo-tip-driver displacements have been previously calibrated from the topographs of Si(111)- (7×7) reconstruction. Two steps are visible in the figure; of the three terraces, only the one in the center is well ordered. More than 80% of surface was usually found to be disordered, despite the appearance of the typical streaky (1×2) LEED pattern. Patches of (2×1) or (1×2) structure were sometimes observed in the disordered areas. In the

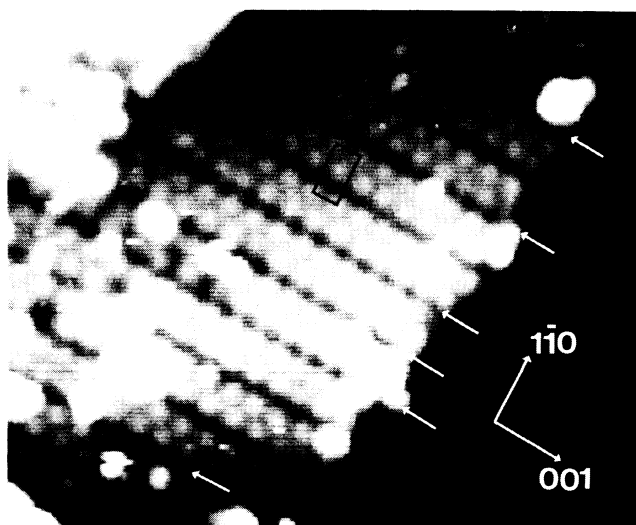


FIG. 1. $240 \times 190\text{-}\text{\AA}^2$ gray-scale topograph of Ni(110)-H(5 \times 2). A unit cell of the reconstruction is shown. Antiphase boundaries are indicated by arrows. Dark area at lower right is a disordered lower terrace.

ordered area, a (5 \times 2) structure, as indicated in Figs. 1 and 2, was most frequently found. The average size of a (5 \times 2)-ordered domain was 1000 \AA along the $\langle 1\bar{1}0 \rangle$ and 100 \AA along the $\langle 001 \rangle$ directions. For a typical coherence length in LEED of a few hundred angstroms, the streaks along the $\langle 001 \rangle$ in the LEED pattern can thus be readily understood. Several types of defects were observed, including missing first-layer atoms, dislocations along the $\langle 001 \rangle$, and antiphase boundaries. Introducing impurity gases (CO or CH₄) increased the defect density, effectively destroying the ordered structure after exposure of ≈ 100 L.

Figure 2(a) shows a $120 \times 95\text{-}\text{\AA}^2$ STM topograph of the Ni(110)-H(5 \times 2) structure. Schematic diagrams of the Ni(110)-(1 \times 1) and Ni(110)-H(5 \times 2) structures observed by STM are shown in Figs. 3(a) and 3(b), respectively. In the (5 \times 2) structure, all the first-layer Ni atoms are laterally displaced by 0.5 \AA along the dimerizing direction, as indicated by arrows in Fig. 3(b), forming tetramers. The lateral displacement agrees with the 0.5- \AA first-layer average displacement determined recently by ion channeling.¹⁶ When the STM tip was sufficiently sharp, the tetramer, seen as a single blob in the scan of Fig. 1, could be resolved into four distinct atoms arranged in a square, 2.5 \AA on a side, as in Fig. 2(a). The tetramers are separated by $2d_{\text{Ni}100}$ along the $\langle 001 \rangle$ and $5d_{\text{Ni}110}$ along the $\langle 1\bar{1}0 \rangle$, with every fifth $\langle 001 \rangle$ row missing, making the reconstruction a combination of row pairing and missing rows. Note that the missing row is not along the $\langle 1\bar{1}0 \rangle$, as proposed earlier.¹² The small domain size along the $\langle 001 \rangle$ may be related to the fact that the missing $\langle 001 \rangle$ row requires mass transfer and is

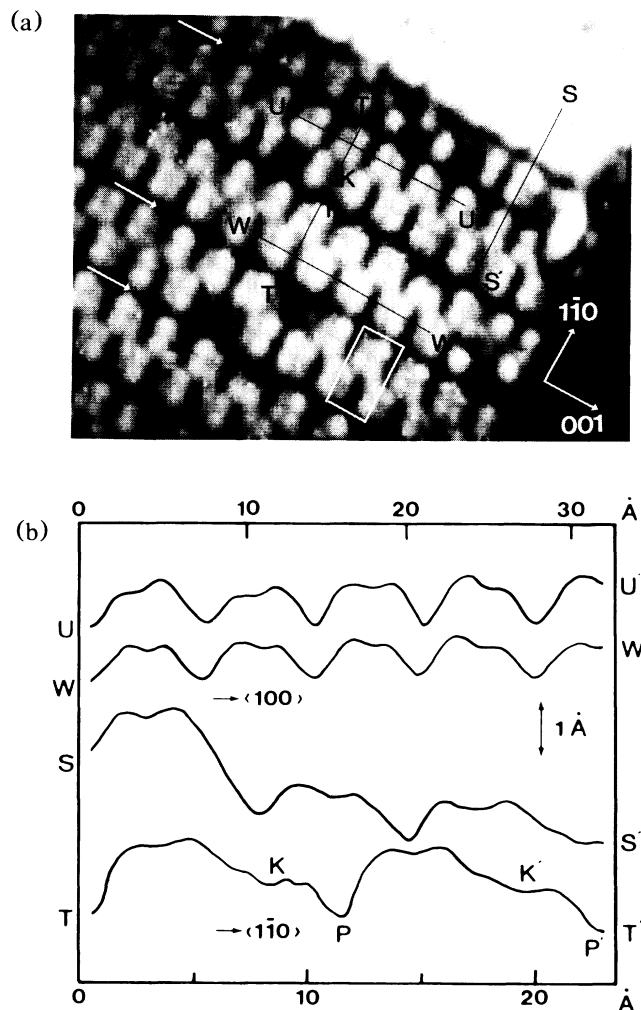


FIG. 2. (a) $120 \times 95\text{-}\text{\AA}^2$ topograph of Ni(110)-H(5 \times 2) reconstruction. A unit cell of the reconstruction is shown. Antiphase boundaries are indicated by arrows. (b) Cross-sectional contours along the lines UU' , WW' , SS' , and TT' in (a). The upper length scale is for the UU' and WW' contours, and the lower scale for the SS' and TT' .

therefore kinetics limited.^{8,15,19} The missing row very frequently forms an antiphase boundary, as can be seen in Figs. 1 and 2(a). In the presence of two or three consecutive antiphase boundaries, the local structure becomes (10 \times 2) or (15 \times 2). In addition, the presence of dislocations with a $\langle 1\bar{1}0 \rangle$ slip direction also changes the local ordered structures. The resultant high defect density substantially destroys the long-range order so that distinct, unstreaked fractional-order LEED spots along the $\langle 1\bar{1}0 \rangle$ direction are rarely visible.

Since the 2.5- \AA separation of tetramer atoms is exactly the Ni nearest-neighbor distance, it seems certain that the STM scans were indeed measuring Ni atomic positions. The other possibility, that the STM is actually

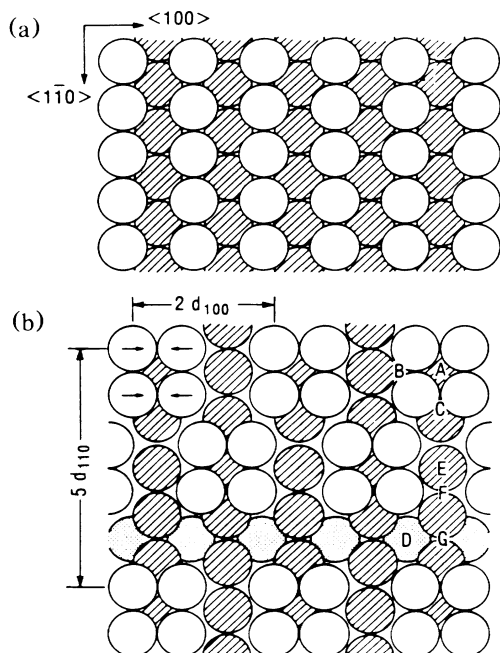


FIG. 3. Schematic of surface structure for (a) unreconstructed Ni(110)-(1 \times 1) and (b) Ni(110)-H(5 \times 2), where open circles represent the first-layer Ni atoms, shaded circles the second layer, and dotted circles the third layer.

sensing H atoms, can be ruled out since a H tetramer is so unlikely.^{9,10} [It is interesting to compare this with the Ni(110)-O case,²⁰ in which the substrate does not reconstruct while the O forms a (2 \times 1) lattice gas; for this system, the STM scan was a map of the adsorbate.] It is possible, however, to get some information about the position of H on the surface by examination of the measured contours for unusual features.

The contours shown in Fig. 2(b) were measured along the corresponding lines of Fig. 2(a). The vertical scale is calibrated from the height of the step along line SS' . The TT' contour includes positions corresponding to $ACEFG$ in Fig. 3(b) and therefore shows high points over the tetramer, a drop down (at K and K') to the second layer between tetramers, and another drop down (at P and P') when the tip is still over the second layer but at the missing-row position (G). The apparent difference in height between points K and P could be due to barrier-height changes (shown in Fig. 4) or to buckling of the second layer at K ,¹⁴ since a constant-current STM scan is always a convolution of electronic and geometric information. The double bumps produced as the tip passed over pairs of Ni atoms, clearly seen in contours UU' and WW' , often showed an asymmetry in height. Hamann has shown that the local charge density can be changed by the presence of hydrogen in the low-temperature Ni(110)-(2 \times 1) system,²¹ so that this asymmetry may be an indication of the presence of H atoms



FIG. 4. (a) 64 \times 124-Å² constant-current topograph taken simultaneously with (b) a work-function image.

in some of the low-symmetry bridge sites designated B in Fig. 3(b). (The heights would be symmetric if B sites on both sides of the tetramer were occupied.) Although other sites (A , C , E , F , and G) have been suggested for H chemisorption, no localized features that could be identified as hydrogen in those sites were present in the STM scans.

An earlier measurement²² found that the work function increased by 0.5 eV after H exposure. The change of the local barrier height can be measured simultaneously with topography by STM by our modulating the tip-sample separation faster than the position feedback can respond and measuring the resultant change in current.²³ Figure 4 shows (a) a topographic image and (b) the corresponding barrier-height image. The barrier height is higher along the missing $\langle 001 \rangle$ row by about 0.3–0.4 eV. It is possible that additional adsorption positions along the missing row, such as the bridge sites in the second layer suggested by electron-energy-loss spectroscopy,^{9,10} result in a higher barrier height.

In summary, we have presented a direct image of chemisorption-induced reconstruction of Ni(110). The structure at room temperature is (5 \times 2), formed by a combination of row pairing and missing $\langle 001 \rangle$ rows. The small domain size along the $\langle 001 \rangle$ and frequent anti-phase boundaries and dislocation explain the observed streaky (1 \times 2) LEED pattern. The position of hydrogen is not determined, but the asymmetric measured heights of the Ni atoms suggest that H atoms may occupy some of the low-symmetry bridge sites.

The authors acknowledge helpful discussions with D. R. Hamann and W. L. Brown. The work of one of us (H.Q.N.) was partially supported by U.S. Office of Naval Research Grant No. NO-0014-86K-0160.

(a)Resident visitor from The Pennsylvania State University, University Park, PA 16802.

¹E. G. Bauer, in *Phase Transition in Surface Films*, edited by J. G. Dash and J. Ruvalds (Plenum, New York, 1980), p. 267, and references therein.

²P. Nordlander, S. Holloway, and J. K. Norskov, *Surf. Sci.*

136, 59 (1984).

³L. H. Germer and A. U. MacRae, *J. Chem. Phys.* **37**, 1382 (1962).

⁴C. W. Tucker, *Surf. Sci.* **26**, 311 (1971).

⁵T. N. Taylor and P. J. Estrup, *J. Vac. Sci. Technol.* **11**, 244 (1974).

⁶V. Penka, K. Christmann, and G. Ertl, *Surf. Sci.* **136**, 307 (1984).

⁷K. H. Rieder and T. Engel, *Phys. Rev. Lett.* **43**, 373 (1979), and **45**, 824 (1980), and *Surf. Sci.* **109**, 140 (1981).

⁸K. Christmann, F. Chehab, V. Penka, and G. Ertl, *Surf. Sci.* **152-153**, 356 (1985).

⁹N. J. Dinardo and E. W. Plummer, *Surf. Sci.* **150**, 89 (1985).

¹⁰M. Jo, M. Onch, and M. Nishijima, *Surf. Sci.* **154**, 417 (1985).

¹¹J. E. Demuth, *J. Colloid Interface Sci.* **58**, 184 (1977).

¹²G. J. R. Jones, J. H. Onuferko, D. P. Woodruff, and B. W. Holland, *Surf. Sci.* **147**, 1 (1984).

¹³K. Griffiths, P. R. Norton, J. A. Davies, W. N. Unertl, and

T. E. Jackman, *Surf. Sci.* **152-153**, 374 (1985).

¹⁴G. Kleine, V. Penka, R. J. Behm, and G. Ertl, *Phys. Rev. Lett.* **58**, 148 (1987).

¹⁵K. Christmann, V. Penka, R. J. Behm, F. Chehab, and G. Ertl, *Solid State Commun.* **51**, 487 (1984).

¹⁶E. Sailer and C. Varelas, *Nucl. Instrum. Methods Phys. Res., Sect. B* **2**, 326 (1984).

¹⁷G. Binnig, H. Rohrer, Ch. Gerber, and E. Weibel, *Appl. Phys. Lett.* **41**, 178 (1982), and *Phys. Rev. Lett.* **50**, 120 (1983).

¹⁸Y. Kuk and P. J. Silverman, *Appl. Phys. Lett.* **48**, 1597 (1986).

¹⁹For example, in the missing-row model of the Au(110), by H. P. Bonzel and S. Ferrer, *Surf. Sci.* **118**, L263 (1982).

²⁰A. M. Baro, G. Binnig, H. Rohrer, Ch. Gerber, E. Stoll, A. Baratoff, and F. Salvan, *Phys. Rev. Lett.* **52**, 1304 (1984).

²¹D. R. Hamann, *Phys. Rev. Lett.* **46**, 1227 (1981).

²²K. Christmann, O. Schober, G. Ertl, and M. Neuman, *J. Chem. Phys.* **60**, 4528 (1974).

²³G. Binnig and H. Rohrer, *Surf. Sci.* **126**, 236 (1983).

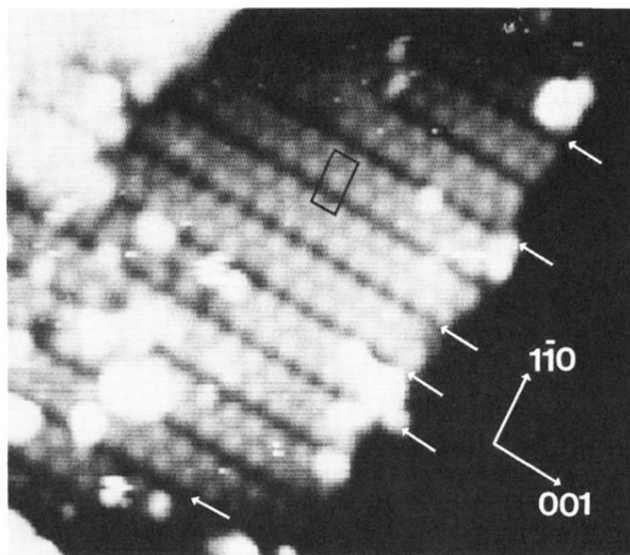


FIG. 1. $240 \times 190\text{-}\text{\AA}^2$ gray-scale topograph of Ni(110)-H(5 \times 2). A unit cell of the reconstruction is shown. Anti-phase boundaries are indicated by arrows. Dark area at lower right is a disordered lower terrace.

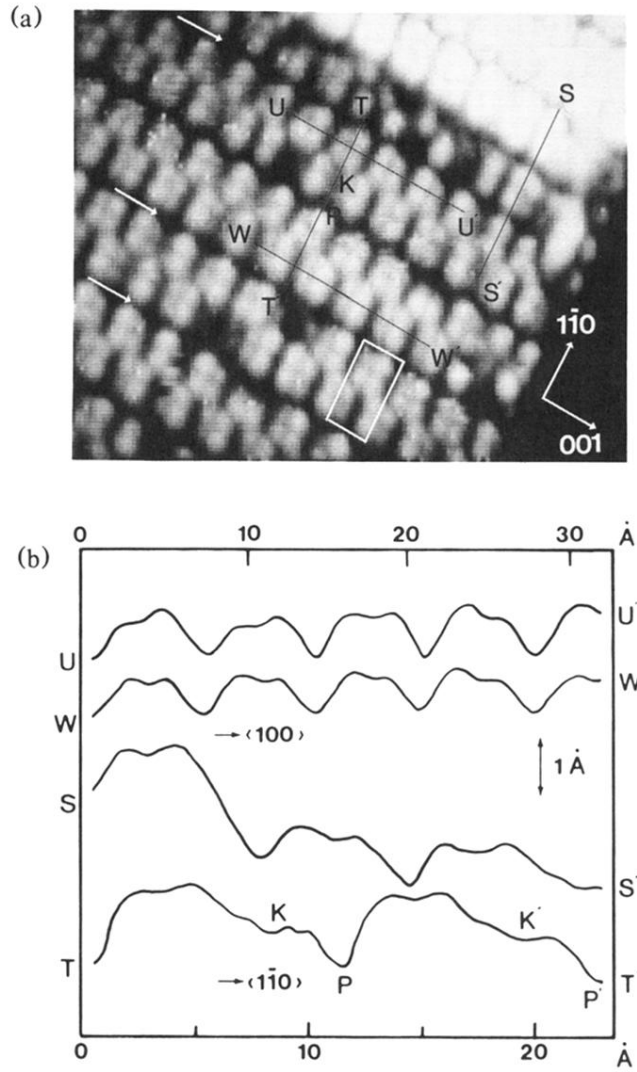


FIG. 2. (a) $120 \times 90\text{-}\text{\AA}^2$ topograph of Ni(110)-H(5×2) reconstruction. A unit cell of the reconstruction is shown. Antiphase boundaries are indicated by arrows. (b) Cross-sectional contours along the lines UU' , WW' , SS' , and TT' in (a). The upper length scale is for the UU' and WW' contours, and the lower scale for the SS' and TT' .

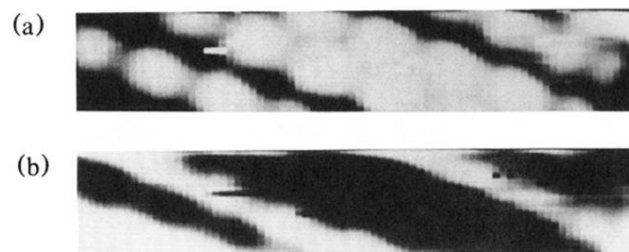


FIG. 4. (a) $64 \times 124\text{-\AA}^2$ constant-current topograph taken simultaneously with (b) a work-function image.